International Journal of Concrete Structures and Materials

Open Access

Property Assessment of High-Performance Concrete Containing Three Types of Fibers

Hua Huang[1,2], Yujie Yuan[2*], Wei Zhang[3*] and Liang Zhu[2]

Abstract

This study investigated the mechanical properties and the effects of the volume fraction for carbon fibers (CF-VF), polypropylene fibers (PPF-VF) and aramid fibers (AF-VF) with a fixed aspect ratio of 650 for the carbon fibers, 400 for the polypropylene fibers and 900 for the aramid fibers in hybrid fiber-reinforced concrete (HFRC). Furthermore, compressive, splitting tensile and flexural tensile tests were carried out to obtain the optimal total volume fraction for the three types of fibers, as well as the optimal ratio between the CF-VF, PPF-VF and AF-VF. In addition, stress–strain curves of normal concrete and HFRC were examined to explore the whole mechanical process. The results indicated the CF-VF, PPF-VF and AF-VF have a significant effect on the tensile and flexural strengths of HFRC. The HFRC with a fiber additional ratio of 25:50:25 had the best hybrid effect. Moreover, a calculation method based on the compressive strength of normal concrete and HFRC and the volume fraction is proposed to calculate the strength of HFRC in engineering as a reference. Besides, a uniaxial compression constitutive mathematical model of normal concrete and HFRC is established.

Keywords: fiber, high-performance concrete, mechanical properties, stress–strain, model

1 Introduction

Many efforts have been made to enhance the mechanical properties of concrete, while the concrete incorporated the fiber is an excellent option to obtain this goal. Ample studies have been conducted in the field of hybrid fiber-reinforced concrete (HFRC), and claim that significant improvement in the performance of HFRC, especially in tensile properties, crack resistance, ductility, and toughness is achieved by incorporating fibers (Bolooki Poorsaheli et al., 2021; Chang et al., 2020; Huang et al., 2019; Nassani, 2020; Scorza et al., 2021; Sujay et al., 2020). Therefore, many types of fibers are widely utilized in engineering.

The performance of HFRC is mainly controlled by the key factors of fibers, such as the type of fibers, the elastic modulus of fibers, the volume fraction, and the aspect ratio (Chella Gifta & Prabavathy, 2018). Chella et al. (2018) studied the energy absorption capacity, compressive strength, and split tensile strength of steel polyester hybrid fiber-reinforced concrete. The results reported that the mechanical properties, energy absorption capacity, and modulus of rupture were significantly improved due to the positive hybrid effect between two different fibers, while the increase of fiber volume fractions marginally improved the compressive strength. Xu et al. (2018) examined the stress–strain behavior and damage evolution of steel-polypropylene-reinforced concrete. The effects of different fiber types, volume fractions, and aspect ratios were investigated through the uniaxial cyclic compression and tension tests (Alimohammadi et al., 2019, 2020). The results revealed that the mechanical behavior of HFRC was significantly improved by the fiber hybrid effect. Moreover, the peak strength, peak strain, toughness, and post-peak ductility of the HFRC under tension and compression were improved, and the stiffness degradation and damage accumulation were

*Correspondence: 15029287701@163.com; zhangwei621@gmail.com
[2] School of Civil Engineering, Chang'an University, Xi'an 710061, China
[3] School of Civil Engineering, Fujian University of Technology, Fuzhou 350118, China
Full list of author information is available at the end of the article

Huang *et al. Int J Concr Struct Mater*   (2021) 15:39

Page 2 of 17

alleviated with the increase of volume fractions for the steel and polypropylene fibers. Koniki et al. (2019) analyzed the effect of metallic (steel) and nonmetallic (polyester and polypropylene) fibers on HFRC. They reported that the improvements in the tensile strength and toughness of the HFRC were attributed to the addition of the synthetic fibers in the concrete matrix. Balcikanli et al. (2020) systematically studied the hybrid effects of steel, synthetic, polypropylene, and glass on the flexural and compressive strength, and pull-out load. It concluded that the pull-out load of the hybrid fiber concrete with a maximum 2% total fiber ratio was increased 75.1% compared with common concretes, and was the largest increase among all specimens. However, the specimen with a 1% total fiber ratio and 73.9% increase was the best improvement. It was mainly due to that concrete with excessive fiber density has almost no fluidity and is difficult to put into the mold. Scorze et al. (2021) explored the fracture properties of hybrid fiber-reinforced concrete, involving six types of fibers, such as long straight steel fibers (S35), short straight copper-coated steel fibers (S13), macro-synthetic twisted bundle polypropylene fibers (PP38), macro-synthetic twisted bundle polypropylene fibers (PM20), macro-synthetic monofilament polymer fibers (PP20), and macro-synthetic fibrillated polypropylene fibers (PP12). It found that specimens with S35 showed the best facture toughness, post-peak, and load bearing performance compared to specimens with PM20, S35–PP20, S35–PP12, S13–PP38, and S13–PM20, while the specimen with PM20 has shown the worst performances. In general, the addition of steel fibers in concrete can considerably enhance overall mechanical properties, such as the tensile strength, compressive strength, toughness, and energy absorption capability (Köksal et al., 2013; Tadepalli et al., 2013; Thomas & Ramaswamy, 2007). Moreover, steel fibers tend to have a positive hybrid effect on HFRC with other kinds of fibers (Koniki & Prasad, 2019; Song & Yin, 2016). Although there are abundant advantages from steel fibers in concrete, it is necessary to address the following problems: corrosion, high volumetric density, and the effect on magnetic and electric fields (Balcikanli Bankir & Sevim, 2020; Bolooki Poorsaheli et al., 2021; Chang et al., 2020; Cui et al., 2020; Dawood & Ramli, 2012; Erdem, et al., 2020; Scorza et al., 2021).

Considering the aforementioned questions, it is an excellent choice to adopt synthetic fibers or natural fibers as good substitutes. From previous studies, both synthetic fibers and natural fibers, such as polypropylenes, polymers, carbon, glass, and basalt fibers, are characterized by long-term durability in a corrosive environment due to their excellent chemical stability and hydrophobicity (Bolat et al., 2014; Fidelis et al., 2016; Kakooei et al.,

2012). Hsie et al. (2008) developed the HFRC with coarse monofilament and staple polypropylene fibers, and the effects of the fiber volume fraction on compressive strength, splitting tensile strength, and flexural properties were discussed. The results indicated that the overall mechanical properties of polypropylene HFRC were better than the properties of single fiber-reinforced concrete. The function of monofilament fibers was similar to that of steel fibers when the volume fraction was high enough. Wang et al. (2019) studied the influences of single basalt fibers, single polypropylene fibers, and hybrid fibers with different volume fractions on compressive, splitting tensile and flexural strengths and the stress–strain curve of HFRC. They reported that single-fiber concrete only improved the flexural and splitting tensile strengths, while the hybrid-fiber concrete enhanced the overall performance. Meanwhile, the volume fraction can significantly enhance the strength of single-fiber concrete, whereas the different volume fraction of hybrid fibers can emerge positive or negative synergy effects. Sadrinejad et al. (2018) studied the hybrid effect of polyolefin and polypropylene fibers, which enhanced the compressive and tensile strengths. Nevertheless, excessive fiber content can cause a negative fiber hybrid effect. Hari et al. (2019) found that when self-compacting concrete incorporated sisal-Nylon and hybrid fibers, its flexural and tensile performance was improved. Moreover, the concrete had a certain water absorption capacity to prevent fiber deterioration and guarantee concrete durability. Sujay et al. (2020) evaluated the compressive, flexural, and tensile strength of basalt-PVA fiber-reinforced concrete and claimed that the axial tensile strain capacity increased by approximately 3% compared with common concrete. The concrete cooperating with hybrid non-alloy fiber can trigger high compressive, flexural, and tensile strength, while the excessive fiber volume fraction will emerge negative hybrid effect on the mechanical behaviors of hybrid fiber concrete (Bolooki Poorsaheli et al., 2021; Hsie et al., 2008; Kakooei et al., 2012; Li et al., 2018; Nassani, 2020; Shi et al., 2020; Song & Yin, 2016; Sujay et al., 2020).

2 Research Significance

Previous studies (Balcikanli Bankir & Sevim, 2020; Bolooki Poorsaheli et al., 2021; Caggiano et al., 2016; Cui et al., 2020; Jalal et al., 2017; Koniki & Prasad, 2019; B. Li et al., 2018; Metiche & Masmoudi, 2013; Scorza et al., 2021; Shi et al., 2020; Smarzewski, 2019; Sujay et al., 2020) indicated that the enhancement in the compressive and flexural strengths of HFRC was always strengthened by high-elastic modulus fibers, while the tensile strength was mainly attributed to the low elastic modulus fibers. Whether the utilization of natural or synthetic fibers

Huang *et al. Int J Concr Struct Mater*   (2021) 15:39

Page 3 of 17

with superior durability and high temperature resistance can generate the effect of steel fibers in concrete, thus avoiding the corrosion and high density of steel fibers, especially in marine engineering. Hence, high-elastic modulus fibers (carbon fibers and aramid fibers) and low-elastic modulus polypropylene fibers were all utilized in this paper (Fig. 1). Besides, concrete cooperated with various properties of fibers can enhance the performance of different aspects for the concrete. The abovementioned reviews mainly focus on two types of mixed-fiber concrete without steel fibers, the properties of which are better than those with single-type fibers. Whether multiple fibers in concrete will emerge better hybrid effects needs further study. Few studies have involved the HFRC with three types of fibers without steel fibers. Therefore, it is fundamental to investigate the mechanical properties of HFRC incorporated three types of fibers to obtain the optimal total volume fraction for the three types of fibers, as well as the optimal volume fraction ratio between the three types of fibers.

3 Experimental Program

Previous studies have indicated that the improvement of HFRC properties is mainly attributed to the fiber properties and the volume fraction. Moreover, Hua et al. (2005) (Huang et al., 2019) and Zhu (2019) inspected the effect of carbon fiber aspect ratio of 650, aramid fiber aspect ratios of $500 \sim 1100$, and polypropylene fiber aspect ratios of $300 \sim 620$ on the mechanical properties of HFRC. The results revealed that the specimen with carbon, aramid, and polypropylene fibers aspect ratios of 650, 900 and 400, respectively, has the maximum improvement in terms of compressive, split tensile and flexural strength among all the test batches. Therefore, based on the fixed aspect ratios of 650 for carbon fibers, 400 for polypropylene fibers and 900 for aramid fibers in HFRC, the effects of the volume fraction for carbon fibers (CF-VF), polypropylene fibers (PPF-VF) and aramid fibers (AF-VF) on

the mechanical properties of HFRC were investigated. To obtain the optimal additional ratio of fibers, compressive, splitting tensile and flexural tensile tests were carried out. Finally, the stress–strain curves of normal concrete and HFRC were examined to explore the whole mechanical behavior. The details of the specimens are presented in Table 1.

3.1 Materials

An ordinary Portland cement (P. O 42.5) produced by Jidong cement Tongchuan co. LTD was adopted to prepare normal concrete and HFRC. The fine aggregate utilized was Weihe River sand in Shanxi Province with a fineness modulus less than 2.56. Gravels with particle size ranges of $5 \sim 20$ mm were used as coarse aggregates. In addition, tap water was used in the tests. Carbon fibers were fabricated by Nanjing Mancatel Company, polypropylene fibers were manufactured by Shijiazhuang Ruixin Cellulose Co., Ltd, and aramid fibers were produced by Handan Xuanheng Special Fiber Equipment Co., Ltd. Sodium carboxymethylcellulose was adopted as a dispersant with 0.8 times the mass of the fibers. The superplasticizer used in the experiment was a liquid viscous polycarboxylate-type superplasticizer with a water-reducing rate range of $25 \sim 27\%$. The amounts of superplasticizer in the normal concrete and HFRC were 0.2% and 0.5% cement by weight, respectively. The details of the aforementioned materials are shown in Table 2. Specimens were prepared in five replicates for acquiring the accurate testing data.

3.2 Mixing and Curing

The standard compressive strength of 50 MPa and a $55 \sim 70$ mm slump was utilized as the test benchmark concrete. This mix proportion (Table 3) was designed according to the code "Specification for mix proportion design of ordinary concrete" (JGJ 55-2000) and the code

(a) Carbon fibers   **(b)** Polypropylene fiber   **(c)** Aramid fiber

Fig.1 Fibers. **a** Carbon fibers. **b** Polypropylene fiber. **c** Aramid fiber.

Huang *et al. Int J Concr Struct Mater*   (2021) 15:39

Page 4 of 17

Table 1 Detail of specimens.

Influencing factors	Series	Volume fraction (%)	Proportion (%)			Size (mm³)
			CF-VF	PPF-VF	AF-VF	
Volume fraction	C1	0	0	0	0	Compressive and splitting tensile flexural tests cubes: $100 \times 100 \times 100$ Flexural tests specimen: $100 \times 100 \times 400$
	C2	0.12	33.3	33.3	33.3	
	C3	0.24	33.3	33.3	33.3	
	C4	0.36	33.3	33.3	33.3	
	C5	0.48	33.3	33.3	33.3	
	C6	0.60	33.3	33.3	33.3	
Addition ratio among fibers	Z1	0.12	100	0	0	
	Z2	0.12	0	100	0	
	Z3	0.12	0	0	100	
	Z4	0.12	60	20	20	
	Z5	0.12	50	25	25	
	Z6	0.12	40	40	20	
	Z7	0.12	20	60	20	
	Z8	0.12	25	50	25	
	Z9	0.12	40	20	40	
	Z10	0.12	20	40	40	
	Z11	0.12	25	25	50	
	Z12	0.12	20	20	60	
Uniaxial compression tests	C1	0	0	0	0	$100 \times 100 \times 300$
	Z1	0.12	100	0	0	
	Z2	0.12	0	100	0	
	Z3	0.12	0	0	100	
	Z5	0.12	50	25	25	

C1 refers the common concrete

Table 2 Performance index of carbon, polypropylene and aramid fiber.

Fiber type	Density	Diameter	Length	Tensile strength	Bending strength	Modulus of elasticity	Elongation at break	Acid and Alkaline resistance	Resistivity
	(g/cm³)	(µm)	(µm)	(MPa)	(MPa)	(GPa)	(%)		(Ω.cm)
Carbon fiber	1.78	6.9	4225	3422	837	241	1.25	strength	1.4×10^6
Polypropylene fiber	0.91	30.0	12,000	556	–	7	20.00 ± 5.00	strength	7.0×10^{19}
Aramid fiber	1.44	10.0	9000	2842	686	110	4.40	strength	5.0×10^{19}

Table 3 Concrete mix design.

Water	Cement	Gravel	Sand	Super-plasticizer	W/C ratio	Sand ratio
(Kg/m³)	(Kg/m³)	(Kg/m³)	(Kg/m³)	(Kg/m³)	(%)	(%)
196	500	1136	559	1	39	33

" Technical specification for fiber-reinforced concrete structure" (CECS 38-2004).

To equivalently distribute the fiber in concrete matrixes, a ready-mixed cement mortar method was utilized in concrete production. After mixing, the fresh concrete was placed in $100 \times 100 \times 100$ mm³ cube molds, $100 \times 100 \times 400$ mm³ molds and $100 \times 100 \times 300$ mm³ molds. The specimens were removed and transferred to

Huang *et al. Int J Concr Struct Mater*   (2021) 15:39

Page 5 of 17

the laboratory for testing after curing for 28 days with more than 95% humidity and 20 ± 2 °C according to "Method for Testing Mechanical Properties of Common concrete" (GB/T50081-2002).

3.3 Testing Methods

The compressive, tensile and flexural strengths of the concrete were obtained with the Changchun universal hydraulic testing machine according to the standard "Method for Testing Mechanical Properties of Common concrete" (GB/T50081-2002). The test results are shown in Table 4. In addition, all the tests were duplicated five times, and three valid results were selected to ensure the accuracy of the data (GB/T50081-2002).

The constitutive parametric experiments of normal concrete, a single type of fiber concrete and HFRC were conducted using a Changchun universal hydraulic testing machine (Fig. 2). First, the 100 mm-long ferrules were fixed at both ends of the testing block, and

the 100 mm-long iron blocks were placed and bolted tightly around the ferrules. Then, 5 mm away from the two ends of the test block was reserved to prevent the fixture from directly contacting the test machine. After the test block was placed, a Linear Variable Differential Transformer (LVDT) with a range of 50 mm was installed around the test block to obtain the displacement. The displacement control method was utilized corresponding to the sampling frequency of 5 Hz. A loading speed of 0.03 mm/min and a damage sensitivity of 50% were set to collect stress.

4 Results and Discussion

Table 5 summarizes the experimental results in terms of compressive, tensile and flexural strength. TC-R and FC-R represent the ratios of the tensile strength to the compressive strength and the flexural strength to the compressive strength, respectively.

Table 4 Experimental results-1.

Specimen	Compressive strength (MPa)	Mean compressive strength (MPa)	λ_C	Tensile strength (MPa)	Mean tensile strength (MPa)	λ_S	Flexural strength (MPa)	Mean flexural strength (MPa)	λ_f	TC-R (%)	FC-R (%)
C1	65.59	63.70	1.000	2.78	3.36	1.000	5.23	5.81	1.000	5.27	9.12
	63.54			3.34			6.12				
	61.97			3.96			6.07				
C2	60.19	60.77	0.954	4.34	4.04	1.202	6.38	6.81	1.172	6.64	11.20
	62.83			3.81			7.10				
	59.29			3.97			6.95				
C3	59.75	58.99	0.926	3.85	3.78	1.125	7.17	6.90	1.188	6.41	11.69
	59.37			3.79			7.04				
	57.85			3.70			6.49				
C4	57.65	57.58	0.904	3.64	3.81	1.134	7.35	7.07	1.217	6.61	12.27
	56.38			3.88			7.16				
	58.71			3.91			6.70				
C5	58.24	56.37	0.885	3.79	3.88	1.155	6.78	6.96	1.198	6.88	12.34
	54.25			3.93			7.16				
	56.62			3.92			6.95				
C6	52.95	54.91	0.862	3.85	3.88	1.155	7.06	6.88	1.184	7.07	12.53
	56.54			3.88			6.80				
	55.24			3.91			6.78				
Z1	63.01	62.81	0.986	4.05	4.26	1.268	7.17	6.79	1.169	6.78	10.81
	62.16			4.55			6.74				
	63.26			4.18			6.46				
Z2	57.29	59.62	0.936	4.44	4.13	1.229	7.06	6.64	1.143	6.93	11.14
	61.43			4.35			6.04				
	60.14			3.60			6.81				

λ_C refers the ratio of the mean compressive strength of the specimen to the mean compressive strength of common concrete (specimen C1). λ_S is the ratio of the mean tensile strength of the specimen to the mean tensile strength of common concrete (specimen C1). λ_f denotes the ratio of the mean flexural strength of the specimen to the mean flexural strength of common concrete (specimen C1). TC-R is the ratio of the mean tensile strength to the mean compressive strength of specimens. FC-R is the ratio of the mean flexurcal strength to the mean compressive strength of specimens

Huang *et al. Int J Concr Struct Mater*   (2021) 15:39

Page 6 of 17

Fig.2 Loading-schematic diagram.

4.1 Effect of Volume Fraction on the HFRC Mechanical Properties

4.1.1 Effect of the Hybrid Fiber Volume Fraction on the Fluidity of the HFRC

Fig. 3 shows the properties of the HFRC with different volume fractions (0 ~ 0.60%) of hybrid fibers. It can be seen that with an increase in the volume fraction, the fluidity of the HFRC was noticeably reduced. When the volume fraction reached 0.48%, the HFRC exhibited a "dry" phenomenon. The working performances were reduced significantly in pumping concrete and shotcrete. The reasons can be summarized as follows: ① higher concrete strength is mainly dominated by a lower water–cement ratio. Hence, there is less water in the mixing process of C50. ② Carbon fibers are characterized by absorbing water. In the process of concrete mixing, fibers can absorb water from the concrete slurry to reduce the concrete fluidity (Song & Yin, 2016). ③ With increasing volume fraction of fibers, more water needs to be consumed, corresponding to an increase in the amount of the superplasticizer to supplement the water consumption. However, there is a limited effect on its water reduction under saturated superplasticizer, and the water reduction rate is not proportional to the amount of superplasticizer. ④ Fibers also provide additional internal friction, resulting in a reduction in the fluidity of fresh concrete. In other words, small amounts of cement slurry are adsorbed on the surface of the fibers while mixing the fibers into the HFRC. More cement slurry is adsorbed on the surface of the fibers corresponding to the increase in the fiber volume fraction. This phenomenon leads to less free mortar,

which is not enough to wrap the coarse aggregate, thus affecting the workability of the concrete. In addition, the fluidity of the concrete is influenced by the viscous effect of a three-dimensional network structure composed of a large number of fibers in the concrete matrix.

4.1.2 Failure Modes

Fig. 4 shows the failure modes of HFRC with different fiber volume fractions (0 ~ 0.60%). The results show that with increasing fiber volume fractions, small numbers of micro-fractures emerged on the specimen surface and alleviated the peeling failure. This phenomenon is mainly attributed to the fiber bridging effect (Yoo et al., 2017a, 2017b; Yoo et al., 2017a, 2017b). In other words, when the concrete cracks, fibers are embedded in the two cracked concrete matrixes to prevent further concrete cracking. Although fibers change the crack direction results in other minor cracks.

4.1.3 Effect of Hybrid Fiber Volume Fraction on Mechanical Properties

Fig. 5 shows the hybrid fiber volume fraction effectiveness on mechanical properties. The compressive strength of the HFRC decreased approximately linearly with an increase in the hybrid fiber volume fraction. With increasing volume fractions from 0.12 to 0.6%, the compressive strength of the HFRC was reduced by 4.6, 7.4, 9.6, 11.5, and 13.8% by contrast with that of normal concrete. During the mixing procedure of the fibers and concrete, air infiltration resulted in more pores in the concrete matrix (Balcikanli et al.,2020; Bolooki Poorsaheli et al., 2021; Cui et al., 2020; Scorza et al., 2021). This means that the loose construction around the fibers weakens the bonds of the HFRC. However, with the increasing volume fraction of hybrid fibers, the tensile strength and flexural strength of the HFRC show an unusual increase in contrast to the compressive strength. Moreover, the tensile strength and flexural strength increased first and remained almost unchanged with increasing fiber volume fraction. It can be concluded that the fiber content is a crucial influencing factor on the HFRC strength, while its effect is limited with increasing volume fraction, reaching a maximum at 0.12%.

4.1.4 Relationship of the Tensile and Flexural Strengths to the Compressive Strength

The tensile-to-compressive strength ratio (TC-R) is an important material property of concrete for representing the ultimate strain value in uniaxial tension. Furthermore, the flexural-to-compressive strength ratio (FC-R) is also an important parameter to indicate the brittle material mechanics of the concrete. Fig. 6 shows the effect of

Huang *et al. Int J Concr Struct Mater*   (2021) 15:39

Page 7 of 17

Table 5 Experimental results-2.

Specimen	Compressive strength	Mean compressive strength	λ_c	Tensile strength	Mean tensile strength	λ_s	Flexural strength	Mean flexural strength	λ_f	TC-R	FC-R
	(MPa)	(MPa)		(MPa)	(MPa)		(MPa)	(MPa)		(%)	(%)
Z3	61.57	61.92	0.972	3.03	3.55	1.057	7.47	7.30	1.256	5.74	11.79
	62.92			3.67			7.22				
	61.27			3.94			7.21				
Z4	61.87	60.90	0.956	3.49	3.54	1.054	7.13	7.29	1.255	5.81	11.97
	61.42			3.36			7.53				
	59.41			3.78			7.21				
Z5	60.29	60.07	0.943	3.39	3.86	1.149	5.58	6.32	1.088	6.42	10.52
	57.69			4.02			6.44				
	62.23			4.16			6.94				
Z6	57.18	57.33	0.900	3.22	3.21	0.955	4.84	5.17	0.890	5.59	9.01
	59.73			2.98			4.78				
	55.08			3.42			5.89				
Z7	59.52	58.67	0.921	3.74	3.29	0.979	5.22	5.64	0.970	5.60	9.61
	51.85			3.10			6.35				
	64.64			3.05			5.34				
Z8	52.05	52.93	0.831	3.11	3.60	1.071	5.12	5.48	0.943	6.79	10.34
	53.85			3.90			6.12				
	52.89			3.82			5.21				
Z9	56.94	61.02	0.958	3.01	3.14	0.970	7.37	6.73	1.158	5.08	10.89
	60.74			3.24			6.29				
	65.38			3.15			6.53				
Z10	63.08	62.11	0.975	3.99	3.59	1.068	5.50	5.51	0.948	5.78	8.87
	60.21			3.49			5.66				
	63.04			3.30			5.38				
Z11	61.20	62.62	0.983	3.45	4.14	1.232	6.54	6.97	1.200	6.61	11.13
	67.68			4.88			6.77				
	58.98			4.10			7.59				
Z12	65.52	63.13	0.991	4.64	4.12	1.226	7.01	7.49	1.289	6.53	11.87
	64.01			4.02			7.89				
	59.86			3.71			7.57				

the volume fraction (VF) on the TC-R and FC-R of the HFRC. The increase in VF is accompanied by an increase in the TC-R and FC-R. Moreover, with a volume fraction in the range of 0–0.6%, the maximum differences in the TC-R and FC-R are 1.8 and 3.4%, respectively, corresponding to the average growth rates of the TC-R and FC-R compared with that of the normal concrete, which are 27.6 and 31.7%, respectively. This demonstrates that the volume fraction of hybrid fibers has a great effect on the TC-R and FC-R of HFRC. This phenomenon is mainly attributed to that the bond effect between fibers and concrete matrix can effectively resist part of the external force to avoid concrete creaking. After the concrete cracks, the fibers near the cracked part lose their bonding effect with the concrete matrix. Since the length

of the fiber is generally larger than the width of microcracks, the remaining part of the fiber is embedded in the two parts of the cracked concrete matrix to limit the development of the crack (Yoo, et al., 2017a, 2017b; Yoo, et al., 2017a, 2017b).

4.2 Effect of Additional Ratio of Fibers on HFRC Mechanical Properties

4.2.1 Failure Modes of the HFRC Specimens

In the case of the failure modes of HFRC under the different additional ratios of fibers (Fig. 7), there is a significant difference from a single type of fiber concretes, especially in terms of the number of cracks. Fig. 7a, c shows that many cracks appeared on the cube surface under compressive loading. The cube remained whole,
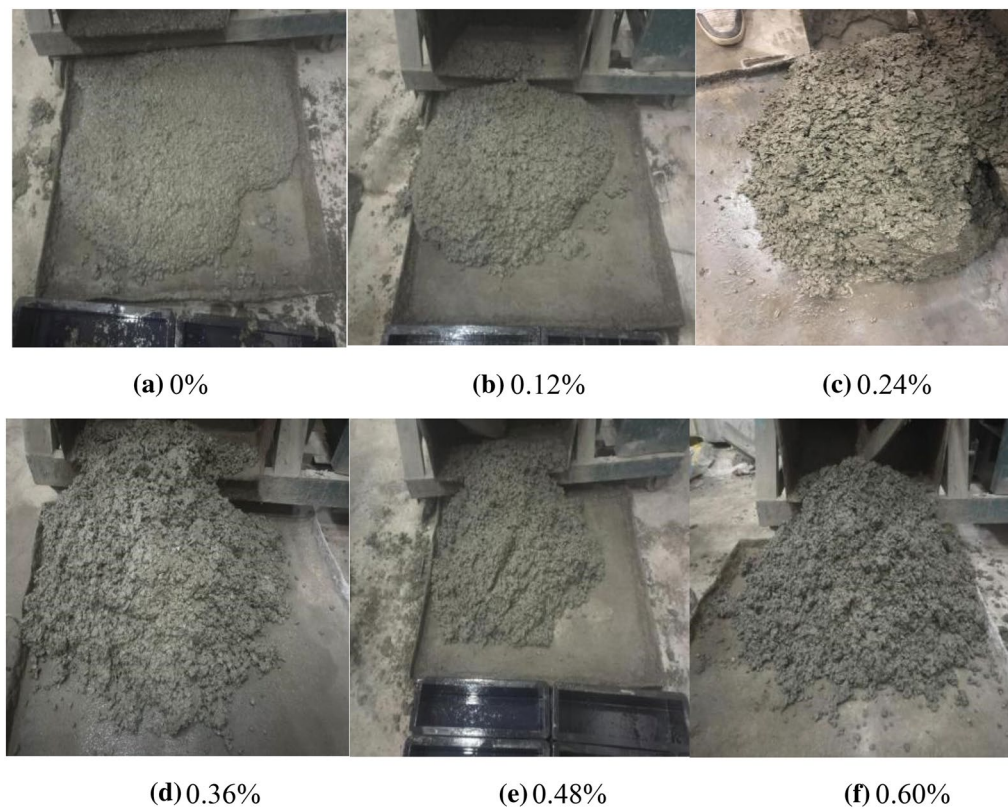
Huang *et al. Int J Concr Struct Mater* (2021) 15:39

Page 8 of 17

Fig.3 HFRC statuses with different fraction volume. **a** 0%. **b** 0.12%. **c** 0.24%. **d** 0.36%. **e** 0.48%. **f** 0.60%.

even though the corner surface of the cube was partially split. However, for Fig. 7b, the spalling was heavier on the surfaces, while there were fewer cracks on the surface compared with those of specimens (a) and (c). This reveals that the crack-resistance behavior of single CF-reinforced concrete and single AF-reinforced concrete is better than that of single PPF-reinforced concrete. This phenomenon is mainly due to the high elastic modulus of the CF and AF. When the concrete is creaked under pressure, those fibers are easily broken or pulled out of the concrete matrix to meet the compressive deformation or cracking of the concrete. As for the PPF with the low elastic modulus and large deformability, it is easily stretched as the concrete is deformed and creaked, thus inhibiting the development and extension of creaks.

After mixing the three types of fibers in the concrete matrix, although some cracks appeared on the surface of the HFRC cubes, the width of the cracks and the surface spalling level were minor compared with those of a single type of fiber-reinforced concrete. Moreover, Fig. 7d, e shows that the surfaces of the specimen (d) appeared only slightly peeling and bulging. This means that the

crack resistance of the HFRC is alleviated by adding the hybrid fibers.

4.2.2 Effect of Hybrid Fiber Volume Fraction on Mechanical Properties

As summarized in Sect. 4.1.3, the optimum volume fraction of hybrid fibers is 0.12%. Therefore, under the different additional ratios of fibers in HFRC and the fixed volume fraction of 0.12%, the relationship of the fiber-to-volume fraction ratio and the HFRC-to-normal concrete strength ratio are investigated and exhibited in Fig. 8. In the case of CF-VF (Fig. 8a), under the same volume fractions of PPF and AF, the tensile strength decreased linearly with decreasing CF-VF and increasing PPF-VF and AF-VF. Meanwhile, the flexural strength decreased to a certain degree. It can be concluded that the strengthening effect of CF-VF on the tensile and flexural strength was weak. The phenomenon was mainly due to the CF adopted in this paper has a small diameter and strong surface adsorption, hence it was difficult to disperse in the concrete matrix, as well as to fully function (Huang et al., 2019; Scorza et al., 2021; Sujay et al., 2020). As PPF-VF (Fig. 8b) decreased and CF-VF and AF-VF increased,
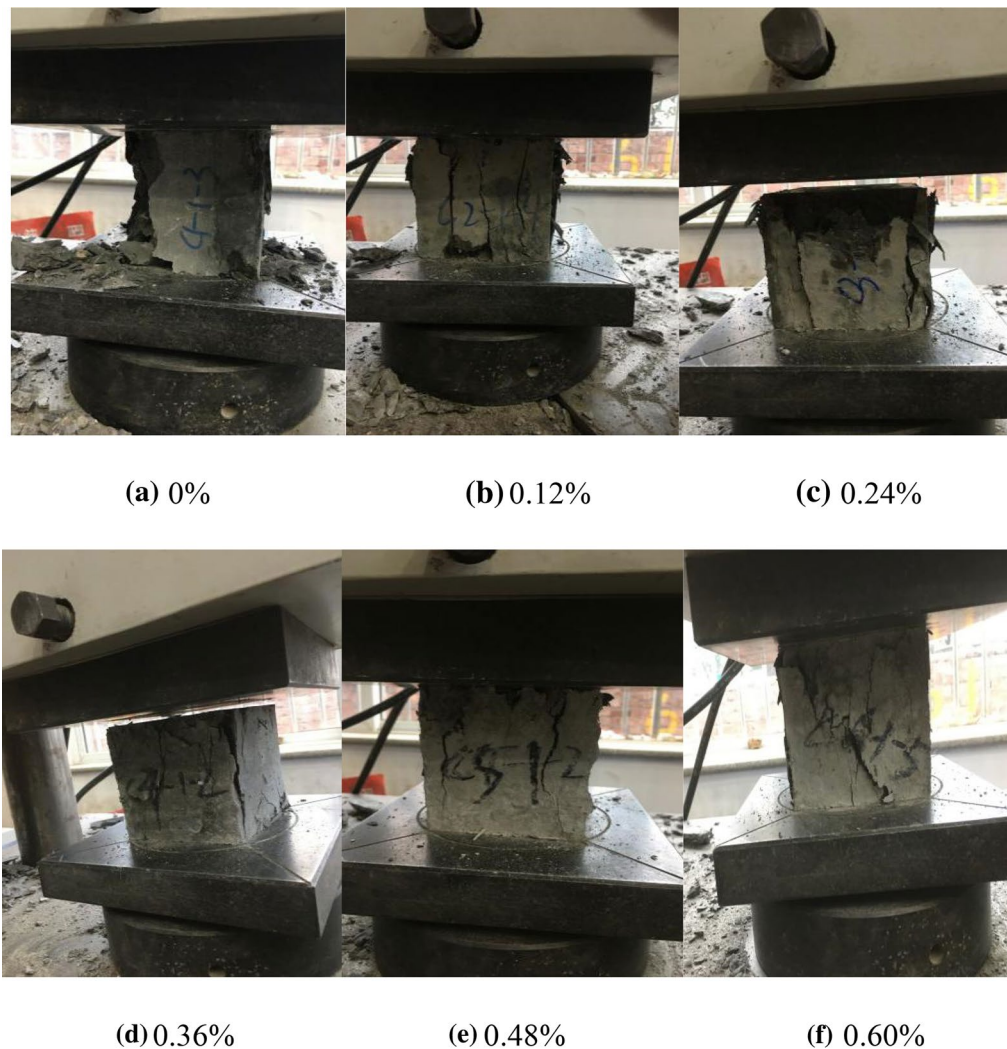
Fig.4 HFRC failure modes with different fraction volume. **a** 0%. **b** 0.12%. **c** 0.24%. **d** 0.36%. **e** 0.48%. **f** 0.60%.
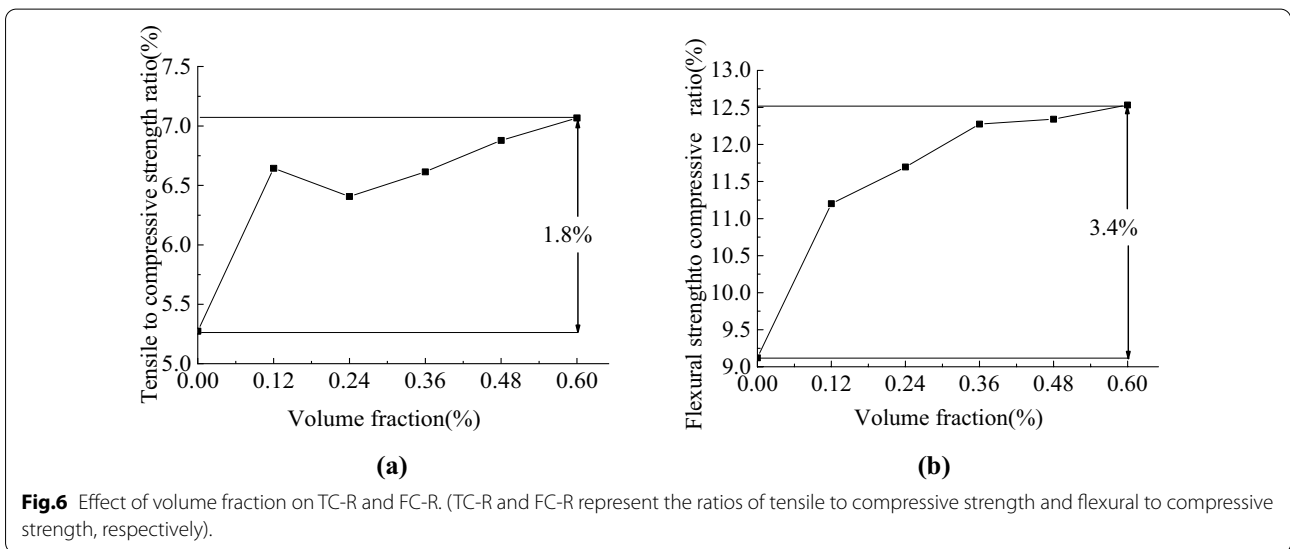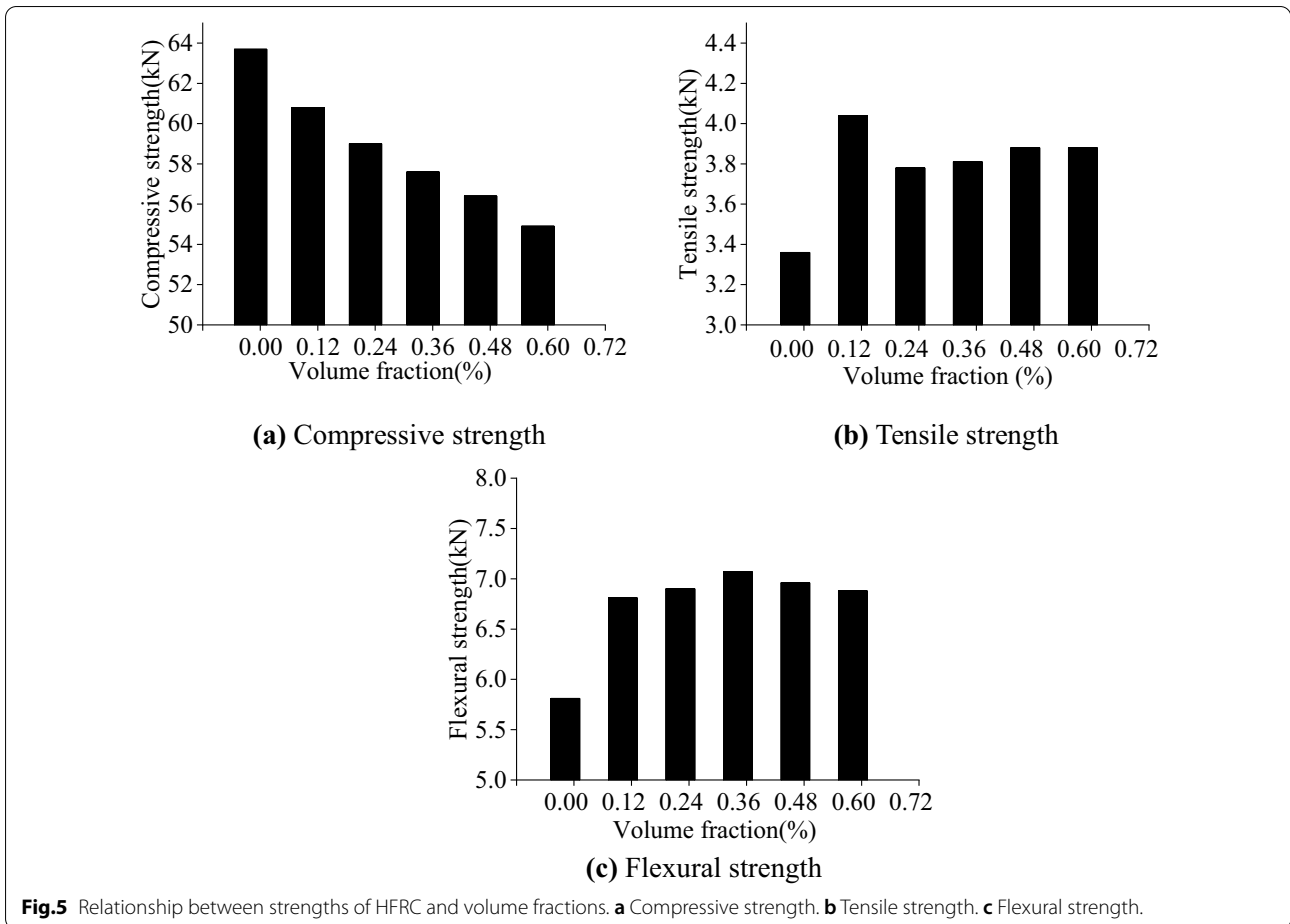
the tensile and flexural strengths reached maximums at a fiber ratio of 25:50:25 and subsequently decreased. In addition, the tensile and flexural strengths decreased first and then decreased with decreasing AF-VF and increasing CF-VF and PPF-VF, reaching a maximum at a fiber ratio of 0:0:100. In general, higher AF-VF with carbon fibers and aramid fibers prone to improve the flexural and tensile strengths of the HFRC, the variation of which is the same as PPF-VF. However, higher CF-VF is prone to negative effects with PPF and AF. The phenomenon is mainly attributed to that AF and PPF are easier to disperse than CF and can exert their role in the concrete matrix (Huang et al., 2019; Scorza et al., 2021; Sujay et al., 2020). Hence, as the PPF-VF and AF-VF change, the overall mechanical properties of HFRC change significantly.

4.3 Stress–Strain Relationship

4.3.1 Characteristics of the Stress–Strain Relationship

The uniaxial compression constitutive relationship is a fundamental property of concrete and an important basis for obtaining the bearing capacity, ductility, strain and stress of concrete structures. The stress–strain curve reflects multiple mechanical properties of concrete. Peak stress represents the compressive strength of concrete prisms. The tangent slope of the curve denotes the elastic modulus of concrete. The area enclosed by the curve indicates the elastoplasticity and toughness of the material.

The axial stress–strain relationship and their characteristic values are shown in Fig. 9 and Table 6, respectively. All the curves contained an ascending stage and two descending stages. The first descending stage refers

Huang *et al. Int J Concr Struct Mater* (2021) 15:39

Page 10 of 17

Fig.5 Relationship between strengths of HFRC and volume fractions. **a** Compressive strength. **b** Tensile strength. **c** Flexural strength.

Fig.6 Effect of volume fraction on TC-R and FC-R. (TC-R and FC-R represent the ratios of tensile to compressive strength and flexural to compressive strength, respectively).

the descending stage close to the ascending stage. However, the descending stage became relatively flat with the increase of the strain. In addition, there was a sharp

decrease as the strain reached to 0.0035με of the normal concrete. The crack resistance of the normal concrete is mainly attributed to the bond between matrixes.

Huang *et al. Int J Concr Struct Mater*   (2021) 15:39

Page 11 of 17

(a) 1:0:0   (b) 0:1:0   (c) 0:0:1

(d) 2:1:1   (e) 1:2:1   (f) 1:1:2

Fig.7 Failure modes based on the variation of additional ratio of fibers (CF: PPF: AF). **a** 1:0:0. **b** 0:1:0. **c** 0:0:1. **d** 2:1:1. **e** 1:2:1. **f** 1:1:2.

Moreover, the bonding force among the concrete matrixes will disappear as the concrete matrix emerges creaks subjected to load. Although there are mechanical bite force and friction between matrixes, the crack resistance is still weak.

In addition, the overall performances of the single type of carbon fiber-reinforced concrete presented the best behavior in contrast to the others, corresponding to the maximum stress at 62.52Mpa. Moreover, the addition of high-elastic modulus fibers, including AF and CF, led to an increase in the concrete compressive strength. The low-elastic modulus fiber (PPF) generated the lowest stress in concrete compressive strength compared with other types of concrete. Meanwhile, the HFRC has the highest energy absorption, and the incorporation of CF in concrete also exerts a great influence on the energy absorption capacities. Nevertheless, the addition of PPF and AF not only cannot improve the energy dissipation capacity of the concrete but also weakens it, especially adding the PPF. Moreover, with the occurrence of cracks in the concrete matrix, the bonding force between the fibers and concrete matrix can consume part of the energy, as well as the bonding force between the fibers and concrete matrix on both sides of the crack. The bond behavior can alleviate crack propagation and mitigate the decreasing rate of stress. In conclusion, CF and hybrid fibers can increase the strength of concrete, as well as the ductility and energy absorption capacities.
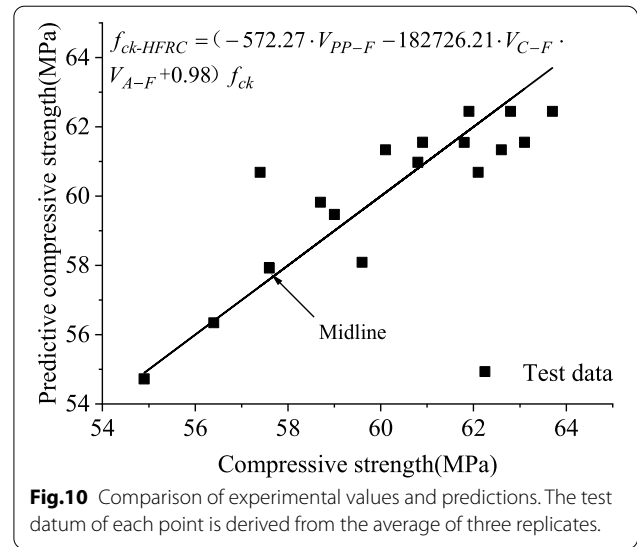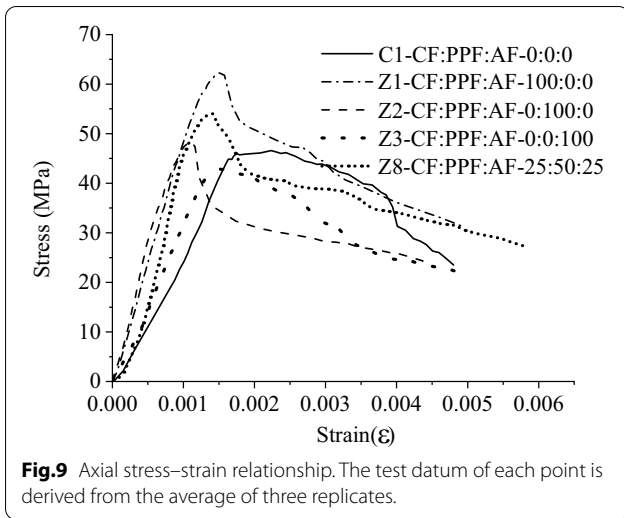
Huang *et al. Int J Concr Struct Mater*   (2021) 15:39

Page 12 of 17
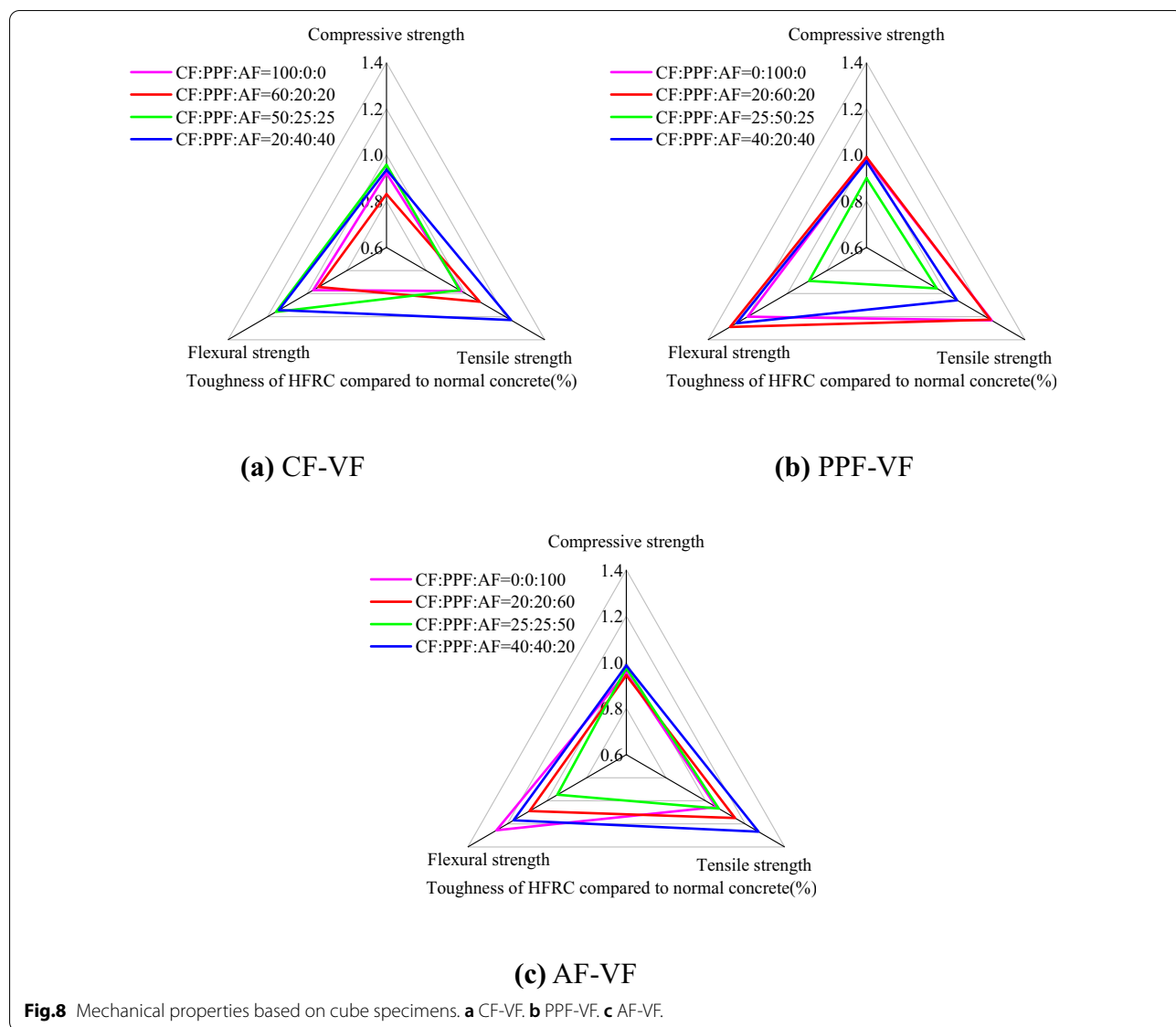
Fig.8 Mechanical properties based on cube specimens. **a** CF-VF. **b** PPF-VF. **c** AF-VF.

4.3.2 Ratio of Peak Stress to the Cubic Compressive Strength

In general, the axial compressive strength is higher than the peak stress because of the higher loading speed and hoop effect in the testing. The peak stress and cubic compressive strengths of all the specimens are exhibited in Table 7.

The $f_{ck}/f_{cu,k}$ values of the five kinds of concrete are between 0.67 and 0.95. Meanwhile, the $f_{ck}/f_{cu,k}$ values of C50 and C60 concrete calculated according to GB50010-2010 are only 0.60 and 0.64, respectively, which are significantly lower than the experimental values. The phenomenon was mainly due to that the transverse expansion of the steel loading plate is smaller than that of the concrete specimen subjected to load. Therefore, the frictional force is emerged on the pressure surface of the concrete specimen, which restrains the transverse expansion of the specimen, thus enhancing the strength of specimens. Besides, the loading end of the axial compressive specimen is restrained to the surrounding and upper of the loading end, while the loading end of the compressive specimen only constrains the upper. Therefore, the transverse expansion constraint of the loading end for the axial compressive specimen is stronger than that of the compression specimen, so the measured concrete strength is also higher.

Fig.9 Axial stress–strain relationship. The test datum of each point is derived from the average of three replicates.

Fig.10 Comparison of experimental values and predictions. The test datum of each point is derived from the average of three replicates.

5 Experimental Analysis

5.1 Correlations Between the Fiber Volume Fraction and Compressive Strength of HFRC

Under a fixed aspect ratio of 650 of the carbon fibers, 400 of the polypropylene fibers and 900 of the aramid fibers, Tables 4, 5, and Figs. 5 and 8 exhibit the interrelation among CF-VF, PPF-VF, AF-VF and the compressive strength of the HFRC. Based on the analysis mentioned above, the multifactor calculation method for determining the HFRC compressive strength is proposed with the influence of three kinds of fiber volume fractions. This formula is as follows:

$$f_{ck\text{-}HFRC} = (-572.27 \cdot V_{PP-F} - 182726.21 \cdot V_{C-F} \cdot V_{A-F} + 0.98)f_{ck}, \quad (1)$$

where $f_{ck\text{-}HFRC}$ and f_{ck} refer to the standard values of HFRC and normal concrete, respectively, and $V_{PP\text{-}F}$, $V_{C\text{-}F}$, and $V_{A\text{-}F}$ denote the volume fractions of the PPF, CF and AF within 0.2%, respectively. The average ratio of the 54 effective test values of the HFRC referring to the calculated values is 0.73 (Fig. 10), and the maximum error is

5.73%. The formulas can be utilized to calculate the compressive strength of the concrete cooperated with CF, PPF, and AF in practical projects as reference.

5.1.1 Prediction of the Compressive Stress–Strain of HFRC and Normal Concrete

The complexity of concrete performance is due to the different properties of the constituent materials and the constraints of external conditions. It is difficult to find a mathematical model that can accurately characterize

Table 7 Peak stress and cubic compressive strength.

Strength	Normal concrete	Carbon fiber concrete	Polypropylene fiber concrete	Aramid fiber concrete	HFRC
$f_{cu,k}$	63.7	62.8	59.6	61.9	63.1
f_{ck}	44.4	59.4	46.2	41.3	51.9
$f_{ck}/f_{cu,k}$	0.70	0.95	0.78	0.67	0.82

$f_{cu,k}$ is the cubic compressive strength, f_{ck} is the axial compressive strength

Table 6 Characteristic values of compressive stress–strain curves.

Specimen	Proportion			Peak stress (MPa)	Peak strain (10^{-4})	Elastic modulus (10^4 MPa)	Energy absorption (kJ/m^3)
	CF-VF	PPF-VF	AF-VF				
C1	–	–	–	46.73	18.06	4.80	157.63
Z1	0.12	–	–	62.52	15.13	4.93	198.18
Z2	–	0.12	–	48.64	11.06	4.37	128.94
Z3	–	–	0.12	43.44	14.88	5.00	143.36
Z8	0.03	0.06	0.03	54.62	14.28	5.78	198.21

(a) Normal concrete

(b) Polypropylene fiber reinforced concrete

(c) Carbon fiber reinforced concrete

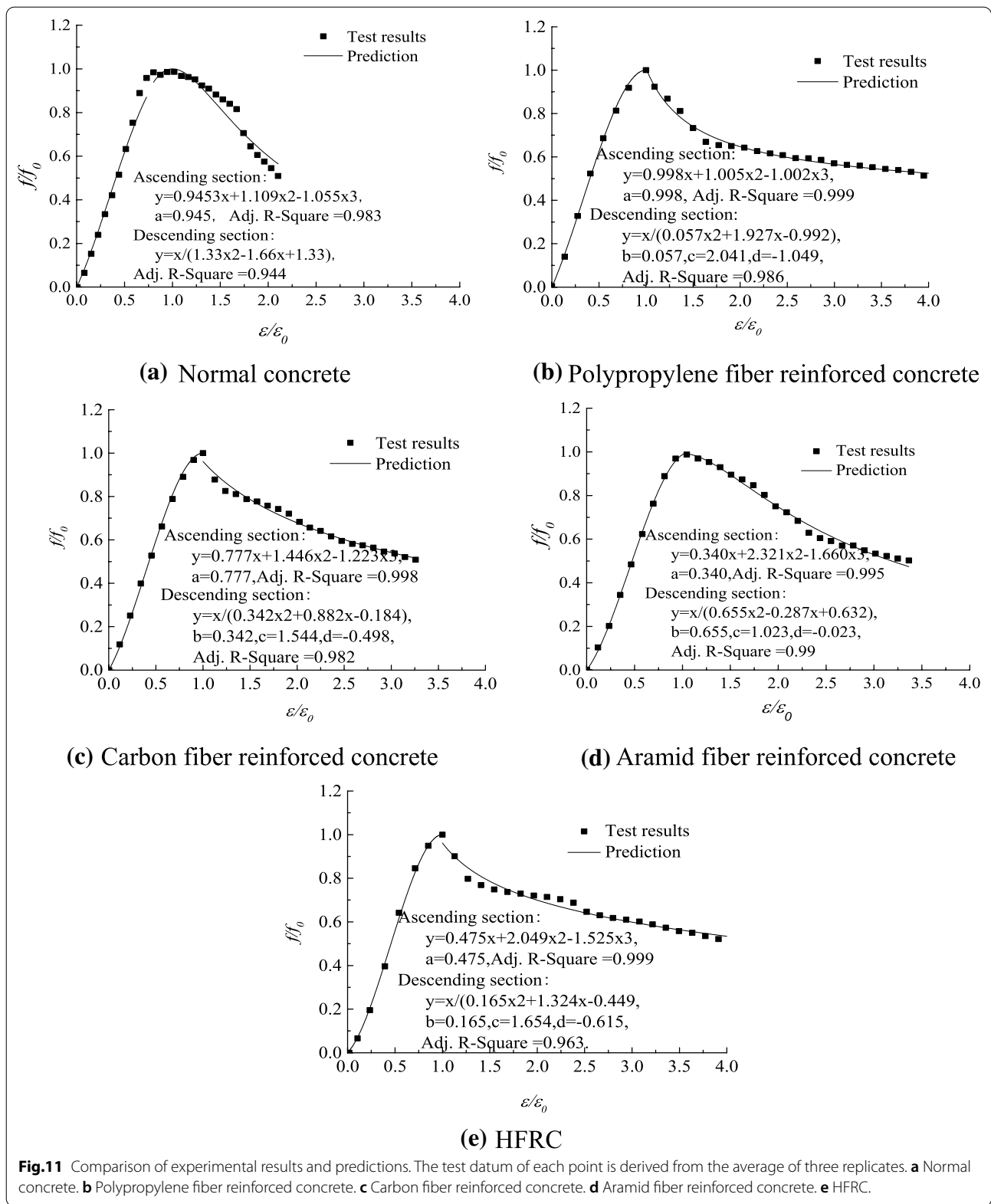**(d)** Aramid fiber reinforced concrete

(e) HFRC

Fig.11 Comparison of experimental results and predictions. The test datum of each point is derived from the average of three replicates. **a** Normal concrete. **b** Polypropylene fiber reinforced concrete. **c** Carbon fiber reinforced concrete. **d** Aramid fiber reinforced concrete. **e** HFRC.

Huang *et al. Int J Concr Struct Mater*   (2021) 15:39

Page 15 of 17

different types of concrete constitutive relation curves. However, the segmented constitutive mathematical model has been proposed by the code for the design of concrete structures (50010–2010, 2010). The theoretical formulas for ascending and descending sections are as follows:

$$\left.\begin{array}{l} y = ax + (3 - 2a)x^2 + (a - 2)x^3, 0 \le x \le 1 \\ y = \dfrac{x}{b(x-1)^2 + x}, x \ge 1 \end{array}\right\}, \quad (2)$$

where $y = \frac{f}{f_0}$ represents the ratio of the test stress to the peak stress; $x = \frac{\varepsilon}{\varepsilon_0}$ denotes the test strain-to-peak strain ratio; a denotes the ratio of the initial elastic modulus to the secant modulus at the peak stress, and b is the plasticity index.

Based on the aforementioned tests and Eqs. (2), (3) can be used to calculate the strain–stress of HFRC and normal concrete:

$$\left.\begin{array}{l} y = ax + (3 - 2a)x^2 + (a - 2)x^3, 0 \le x \le 1 \\ y = \dfrac{x}{b(x-1)^2 + cx + d}, x \ge 1 \end{array}\right\}, \quad (3)$$

where c and d denote the strain adjustment coefficient and plastic coefficient compensation values, respectively.

Equation (3) is used to fit the stress–strain curve of normal concrete, a single type of fiber-reinforced concrete and HFRC (Fig. 9). Fitting curves are shown in Fig. 11. It can be found that there is a good agreement with the experimental values and predicted values.

6 Conclusions

Based on the comprehensive investigation, the following conclusions can be drawn:

(1) The increase in the volume fraction of carbon fiber, aramid fiber, and polypropylene fiber had a positive effect on the tensile and flexural strengths of HFRC. Meanwhile, the compressive strength of the HFRC decreased linearly with increasing hybrid fiber volume fraction. In addition, the splitting tensile strength reached its maximum at 0.12% volume fraction, while the flexural strength first increased and then decreased with increasing hybrid fiber volume fraction, reaching a maximum when the volume fraction is 0.36%. In all, the optimal volume fraction of hybrid fibers was 0.12%.

(2) The additional ratio among fibers generated positive and negative effects on the HFRC properties. The reinforcing effects of the aramid fibers and polypropylene fibers on the concrete strength were better than those of the carbon fiber. The overall mechanical properties of the HFRC with 3 types of fibers were better than those of a single type of fiber-reinforced concrete. Moreover, the HFRC with an additional ratio of fibers of 25:50:25 had the best hybrid effect.

(3) The f_{ck} /$f_{cu,k}$ value of the HFRC was significantly higher than those of the normal concrete and the predicted value by code, specifically in respect of the carbon, polypropylene, and hybrid fibers.

(4) An equation was proposed to predict the HFRC compressive strength for specimens with various volume fractions (0–0.60%) of carbon fibers, aramid fibers, and polypropylene fibers. The equation can be used in practical projects as a reference.

(5) The addition of carbon fibers and hybrid fibers with a fiber ratio of 25:50:25 significantly influenced the energy consumption capacities.

(6) Based on the constitutive theoretical model proposed by previous research, a uniaxial compression constitutive mathematical model of normal concrete and HFRC was established to provide a theoretical basis for the HFRC stress and strain prediction. The calculated values were in good agreement with the testing data.

Authors' information
Hua Huang is a professor at the School of Civil Engineering, Xi'an Technological University, Xi'an, China. Yujie Yuan is a PhD candidate at School of Civil Engineering, Chang'an University, Xi'an, China. Wei Zhang is a professor at the School of Civil Engineering, Fujian University of Technology, Fuzhou, China. Liang Zhu is a graduated Master student from the School of Civil Engineering, Chang'an University, Xi'an, China.

Availability of data and materials
The data sets used and/or analyzed during the current study are available from the corresponding author on reasonable request.

Huang *et al. Int J Concr Struct Mater*   (2021) 15:39

Page 16 of 17

Declarations

Competing interests
The authors declare that they have no competing interests. The authors declare that they have no competing interests.

Author details
[1]School of Civil Engineering, Xi'an Technological University, Xi'an 710021, China. [2]School of Civil Engineering, Chang'an University, Xi'an 710061, China. [3]School of Civil Engineering, Fujian University of Technology, Fuzhou 350118, China.

References

Alimohammadi, H., Lotfollahi-Yaghin, M., & Esfahani, M. (2019). Effects of different parameters on inelastic buckling behavior of composite concrete-filled steel tubes. *International Research Journal of Engineering and Technology, 6*(12), 1–16.

Alimohammadi, H., Dastjerdi, K., & Yaghin, M. (2020). The study of progressive collapse in dual systems. *Civil and Environmental Engineering, 16*(1), 1–7. https://doi.org/10.2478/cee-2020-0009

Balcikanli Bankir, M., & Sevim, U. K. (2020). Performance optimization of hybrid fiber concrete according to mechanical properties. *Construction and Building Materials, 261*(2020), 1–18. https://doi.org/10.1016/j.conbuildmat.2020.119952

Bolat, H., Şimşek, O., Çullu, M., Durmuş, G., & Can, Ö. (2014). The effects of macro synthetic fiber reinforcement use on physical and mechanical properties of concrete. *Composites Part B: Engineering, 61*, 191–198. https://doi.org/10.1016/j.compositesb.2014.01.043

Bolooki Poorsaheli, H., Behravan, A., & Tabatabaei Aghda, S. T. (2021). Durability performance of hybrid reinforced concretes (steel fiber+polyolefin fiber) in a harsh marine tidal zone of Persian Gulf. *Construction and Building Materials, 266*(2021), 1–11. https://doi.org/10.1016/j.conbuildmat.2020.121176

Caggiano, A., Gambarelli, S., Martinelli, E., Nistico, N., & Pepe, M. (2016). Experimental characterization of the post-cracking response in Hybrid Steel/Polypropylene Fiber-Reinforced Concrete. *Construction and Building Materials, 125*(2016), 1035–1043. https://doi.org/10.1016/j.conbuildmat.2016.08.068

CESE 38-2004 (2004). Technical specification for fiber reinforced concrete structure. In. Beijing: China Architecture & Building Press.

Chang, J., Cui, K., & Zhang, Y. (2020). Effect of hybrid steel fibers on the mechanical performances and microstructure of sulphoaluminate cement-based reactive powder concrete. *Construction and Building Materials*. https://doi.org/10.1016/j.conbuildmat.2020.120502

ChellaGifta, C., & Prabavathy, S. (2018). Study on energy absorption capacity of steelpolyester hybrid fiber reinforced concrete under uni-axial compression. *Journal of the Institution of Engineers (india) Series A, 99*(3), 547–553. https://doi.org/10.1007/s40030-018-0310-y

Cui, T., He, H., Yan, W., & Zhou, D. (2020). Compression damage constitutive model of hybrid fiber reinforced concrete and its experimental verification. *Construction and Building Materials*. https://doi.org/10.1016/j.conbuildmat.2020.120026

Dawood, E. T., & Ramli, M. (2012). Mechanical properties of high strength flowing concrete with hybrid fibers. *Construction and Building Materials, 28*(1), 193–200. https://doi.org/10.1016/j.conbuildmat.2011.08.057

Erdem, T. K., Demirhan, S., Yıldırım, G., Banyhussan, Q. S., Şahin, O., Balav, M. H., & Şahmaran, M. (2020). Effects of mixture design parameters on the mechanical behavior of high-performance fiber-reinforced concretes. 32(12), 04020368.

Fidelis, M. E. A., Filho, R. D. T., Silva, F. D. A., Mechtcherine, V., Butler, M., & Hempel, S. (2016). The effect of accelerated aging on the interface of jute textile reinforced concrete. *Cement & Concrete Composites, 74*, 7–15.

GB 50010-2010, (2010). Code for design of concrete structures. China Architecture & Building Press.

Hari, R., & Mini, K. M. (2019). Mechanical and durability properties of sisal-Nylon 6 hybrid fibre reinforced high strength SCC. *Construction and Building Materials, 204*(2019), 479–491. https://doi.org/10.1016/j.conbuildmat.2019.01.217

Hsie, M., Tu, C., & Song, P. S. (2008). Mechanical properties of polypropylene hybrid fiber-reinforced concrete. *Materials Science and Engineering: A, 494*(1–2), 153–157. https://doi.org/10.1016/j.msea.2008.05.037

Hua, Y., Lian, J., & Zhou, T. (2005). Relationship between the mechanical properties of hybrid fiber reinforced concrete and length/ diameter aspect ratio of hybrid fiber[J]. *Journal of Building Materials, 8*(1), 71–76.

Huang, H., Yuan, Y., Zhang, W., & Zhu, L. (2019). Experimental study on the mechanical properties and the microstructure of hybrid-fiber-reinforced concrete under an early stage. *Structural Concrete, 21*(3), 1106–1122. https://doi.org/10.1002/suco.201900262

Jalal, A., Shafiq, N., Nikbakht, E., Kumar, R., & Zahid, M. (2017). Mechanical properties of hybrid basalt-polyvinyl alcohol (PVA) fiber reinforced concrete. Paper presented at the International Symposium on Material Science and Engineering, ISMSE 2017, January 13, 2017–January 15, 2017, Kuala Lumpur, Malaysia.

JGJ 55-2000, (2000). Specification for mix proportion design of ordinary concrete. China Architecture & Building Press.

Kakooei, S., Akil, H. M., Jamshidi, M., & Rouhi, J. (2012). The effects of polypropylene fibers on the properties of reinforced concrete structures. *Construction and Building Materials, 27*(1), 73–77. https://doi.org/10.1016/j.conbuildmat.2011.08.015

Köksal, F., Şahin, Y., Gencel, O., & Yiğit, İ. (2013). Fracture energy-based optimisation of steel fibre reinforced concretes. *Engineering Fracture Mechanics, 107*, 29–37. https://doi.org/10.1016/j.engfracmech.2013.04.018

Koniki, S., & Prasad, D. R. (2019). Influence of hybrid fibres on strength and stress-strain behaviour of concrete under uni-axial stresses. *Construction and Building Materials, 207*, 238–248. https://doi.org/10.1016/j.conbuildmat.2019.02.113

Li, B., Chi, Y., Xu, L., Shi, Y., & Li, C. (2018). Experimental investigation on the flexural behavior of steel-polypropylene hybrid fiber reinforced concrete. *Construction and Building Materials, 191*, 80–94. https://doi.org/10.1016/j.conbuildmat.2018.09.202

Metiche, S., & Masmoudi, R. (2013). Analysis and design procedures for the flexural behavior of glass fiber-reinforced polymer composite poles. *Journal of Composite Materials, 47*(2), 207–229. https://doi.org/10.1177/0021998312438721

Nassani, D. E. (2020). Experimental and analytical study of the mechanical and flexural behavior of hybrid fiber concretes. *Structures, 28*, 1746–1755. https://doi.org/10.1016/j.istruc.2020.10.014

Sadrinejad, I., Madandoust, R., & Ranjbar, M. M. (2018). The mechanical and durability properties of concrete containing hybrid synthetic fibers. *Construction and Building Materials, 178*(2018), 72–82. https://doi.org/10.1016/j.conbuildmat.2018.05.145

Scorza, D., Luciano, R., Mousa, S., & Vantadori, S. (2021). Fracture behaviour of hybrid fibre-reinforced roller-compacted concrete used in pavements. *Construction and Building Materials*. https://doi.org/10.1016/j.conbuildmat.2020.121554

Shi, F., Pham, T. M., Hao, H., & Hao, Y. (2020). Post-cracking behaviour of basalt and macro polypropylene hybrid fibre reinforced concrete with different compressive strengths. *Construction and Building Materials*. https://doi.org/10.1016/j.conbuildmat.2020.120108

Smarzewski, P. (2019). Influence of basalt-polypropylene fibres on fracture properties of high performance concrete. *Composite Structures, 209*, 23–33. https://doi.org/10.1016/j.compstruct.2018.10.070

Song, W., & Yin, J. (2016). Hybrid effect evaluation of steel fiber and carbon fiber on the performance of the fiber reinforced concrete. *Materials*. https://doi.org/10.3390/ma9080704

GB/T50081-2019. (2019). Standard for test method of mechanical properties on ordinary concrete. China Architecture & Building Press.

Sujay, H. M., Nair, N. A., Sudarsana Rao, H., & Sairam, V. (2020). Experimental study on durability characteristics of composite fiber reinforced high-performance concrete incorporating nanosilica and ultra fine fly ash. *Construction and Building Materials, 262*(2020). https://doi.org/10.1016/j.conbuildmat.2020.120738

Tadepalli, P. R., Mo, Y. L., & Hsu, T. T. C. (2013). Mechanical properties of steel fibre concrete. *Magazine of Concrete Research, 65*(8), 462–474. https://doi.org/10.1680/macr.12.00077

Huang *et al. Int J Concr Struct Mater*   (2021) 15:39

Page 17 of 17

Thomas, J., & Ramaswamy, A. (2007). Mechanical properties of steel fiber-reinforced concrete. *Journal of Materials in Civil Engineering, 19*(5), 385–392.

Wang, D., Ju, Y., Shen, H., & Xu, L. (2019). Mechanical properties of high performance concrete reinforced with basalt fiber and polypropylene fiber. *Construction and Building Materials, 197*(2019), 464–473. https://doi.org/10.1016/j.conbuildmat.2018.11.181

Xu, L., Wei, C., & Li, B. (2018). Damage evolution of steel-polypropylene hybrid fiber reinforced concrete: experimental and numerical investigation. *Advances in Materials Science and Engineering*. https://doi.org/10.1155/2018/1719427

Yoo, D.-Y., Kang, S.-T., Banthia, N., & Yoon, Y.-S. (2017a). Nonlinear finite element analysis of ultra-high-performance fiber-reinforced concrete beams.

International Journal of Damage Mechanics, 26(5), 735–757. https://doi.org/10.1177/1056789515612559

Yoo, D.-Y., Kim, S., Park, G.-J., Park, J.-J., & Kim, S.-W. (2017b). Effects of fiber shape, aspect ratio, and volume fraction on flexural behavior of ultra-high-performance fiber-reinforced cement composites. *Composite Structures, 174*, 375–388. https://doi.org/10.1016/j.compstruct.2017.04.069

Zhu, L. (2019). Study on mechanical properties and microscopic mechanism of hybrid fiber modified concrete. (Master), Chang'an University, China.

Publisher's Note